

## The wavelength dependent photovoltaic effects caused by two different mechanisms in carbon nanotube film/CuO nanowire array heterodimensional contacts

Jia Xu, Jia-Lin Sun, Jinquan Wei, and Jinliang Xu

Citation: *Appl. Phys. Lett.* **100**, 251113 (2012); doi: 10.1063/1.4730433

View online: <http://dx.doi.org/10.1063/1.4730433>

View Table of Contents: <http://apl.aip.org/resource/1/APPLAB/v100/i25>

Published by the [American Institute of Physics](http://www.aip.org).

### Related Articles

Non-planar substrate effect on the interface trap capacitance of metal-oxide-semiconductor structures with ultra thin oxides

*J. Appl. Phys.* **112**, 094502 (2012)

Band alignment of epitaxial ZnS/Zn3P2 heterojunctions

*J. Appl. Phys.* **112**, 093703 (2012)

Comparison of tunneling current assisted by neutral and positive traps with finite ranged core-potential

*J. Appl. Phys.* **112**, 094101 (2012)

Design rules of (Mg,Zn)O-based thin-film transistors with high-kWO3 dielectric gates

*Appl. Phys. Lett.* **101**, 183502 (2012)

Impact of atomic layer deposition temperature on HfO2/InGaAs metal-oxide-semiconductor interface properties

*J. Appl. Phys.* **112**, 084103 (2012)

### Additional information on *Appl. Phys. Lett.*

Journal Homepage: <http://apl.aip.org/>

Journal Information: [http://apl.aip.org/about/about\\_the\\_journal](http://apl.aip.org/about/about_the_journal)

Top downloads: [http://apl.aip.org/features/most\\_downloaded](http://apl.aip.org/features/most_downloaded)

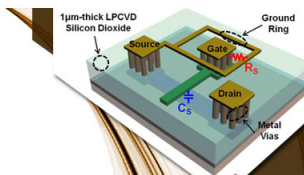
Information for Authors: <http://apl.aip.org/authors>

## ADVERTISEMENT



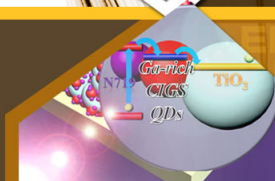
**EXPLORE WHAT'S  
NEW IN APL**

**SUBMIT YOUR PAPER NOW!**



### **SURFACES AND INTERFACES**

Focusing on physical, chemical, biological, structural, optical, magnetic and electrical properties of surfaces and interfaces, and more...



### **ENERGY CONVERSION AND STORAGE**

Focusing on all aspects of static and dynamic energy conversion, energy storage, photovoltaics, solar fuels, batteries, capacitors, thermoelectrics, and more...

## The wavelength dependent photovoltaic effects caused by two different mechanisms in carbon nanotube film/CuO nanowire array heterodimensional contacts

Jia Xu,<sup>1</sup> Jia-Lin Sun,<sup>2,a)</sup> Jinqun Wei,<sup>3</sup> and Jinliang Xu<sup>1,a)</sup>

<sup>1</sup>Beijing Key Laboratory of Low-grade Energy Multiphase Flow and Heat Transfer, School of Renewable Energy, North China Electric Power University, Beijing 102206, China

<sup>2</sup>Department of Physics, State Key Laboratory of Low-Dimensional Quantum Physics, Tsinghua University, Beijing 100084, China

<sup>3</sup>Department of Mechanical Engineering, Key Laboratory for Advanced Materials Processing Technology of Education Ministry, Tsinghua University, Beijing 100084, China

(Received 16 April 2012; accepted 5 June 2012; published online 22 June 2012)

Heterodimensional contacts were fabricated by coating double-walled carbon nanotube (CNT) films on CuO nanowire arrays. Wavelength dependent photovoltaic effects by irradiating the devices with 405, 532, and 1064 nm lasers were observed. Two possible mechanisms responsible for the observed results were discussed. Photoexcitations within CuO nanowires and Schottky barriers in the heterojunctions dominate the photovoltaics in the 405 and 532 nm cases. For the 1064 nm case, the photovoltaic is the result of the excitation within the CNTs and of the heterodimensionality effect. Control experiments on CNT film/CuO granular film heterodimensional contacts further show the relationship between these two mechanisms. © 2012 American Institute of Physics. [<http://dx.doi.org/10.1063/1.4730433>]

Carbon nanotube (CNT) films composed of thousands of randomly distributed CNTs have been demonstrated to be transparent, conductive, and flexible materials, and they can be used as a replacement for indium tin oxide electrodes in many optoelectronic devices.<sup>1–3</sup> Recently, heterojunction (HJ) effects in photovoltaics (PVs) have received much attention for their potential applications in solar cells and photodetectors. In these cases, CNT films were used to contacted with many conventional *n*-type semiconductors, such as *n*-Si wafers and nanowire (NW) arrays,<sup>4–7</sup> CdSe nanobelts,<sup>8</sup> and TiO<sub>2</sub> nanotube arrays.<sup>9</sup> Schottky or *p*-*n* barriers in these HJs can afford built-in electric fields with the directions from the *n*-type semiconductors to the CNT films effectively separating the photoinduced carriers. Thus, when the devices are irradiated by light with energies above the bandgaps of the semiconductors, the photoinduced electrons and holes drift to the *n*-type semiconductors and CNT films, respectively.

Meanwhile, CNTs, as a type of low-dimensional material, can form heterodimensional contacts with films and bulk materials.<sup>10</sup> Photoinduced electrons in heterodimensional contacts tend to be transported from the lower-dimensional materials to the neighboring higher-dimensional materials, which has been termed the heterodimensionality (HD) effect in our previous reports.<sup>11,12</sup> When CNT films are in contact with higher-dimensional *n*-type semiconductors, the transport direction of the photoinduced electrons affected by the HD effect is the same as that for those affected by the HJ effect. Thus, the HD effect cannot be directly observed in these structures, and it has rarely been mentioned for such cases. To directly observe the HD effect in PVs, the built-in electric field in the HJs should be designed to make the photoinduced electrons drift to the CNTs. Choosing *p*-type semiconductors to be in contact with the CNTs may be a simple and effective way of achieving the above goals. However, such structures have not been extensively studied thus far.

CuO is a *p*-type semiconductor with a narrow bandgap (1.2–1.9 eV), making it one of the most attractive and commonly used optoelectronic materials.<sup>13</sup> Recently, various groups have reported on the fabrication of CuO NWs, which are in the form of large-scale, vertically aligned arrays, via the heating of Cu substrates in air.<sup>14–16</sup> This approach is extremely simple and the products can be conveniently combined with other materials to form HJs. Herein, we report on the preparation of CuO NW arrays via thermal oxidation and the fabrication of heterodimensional contacts by transferring thin double-walled CNT (DWCNT) film to the top of the CuO NW arrays. PV effects were observed by irradiating the devices with 405, 532, and 1064 nm lasers. The open-circuit voltages,  $U_{oc}$ , and short-circuit currents,  $I_{sc}$ , obtained in the 1064 nm case were reversed compared with the other two cases. These results can be understood in terms of relationship between two mechanisms: HJ and HD effects. Moreover, control experiments carried out on the CNT film/CuO granular film heterodimensional contacts provide further demonstration of the coexistence of these two mechanisms.

CuO nanostructures were fabricated in an ambient atmosphere by direct oxidation of Cu foils (99.999% purity, 0.2 mm thick, size of 1 cm × 2 cm). Before growth, polished Cu foils were ultrasonically cleaned sequentially in acetone, ethanol, and deionized water. Thereafter, the foils were loaded onto shelves of a box-type muffle furnace. The temperature was raised to 500 °C in 1 h and then kept at that temperature for a set period of time. Two types of samples, with total oxidation times of 5 h and 3 h, respectively, were used in our experiments. Figures 1(a) and 1(b) show field emission scanning electron microscopy (FESEM) images of the

<sup>a)</sup>Authors to whom correspondence should be addressed. Electronic addresses: jlsun@tsinghua.edu.cn and xjl@ncepu.edu.cn.

5 h oxidation time sample with different magnification settings. A high density of NWs, with diameters in the range of 150–200 nm, vertically formed on the substrate. For the sample with oxidation time of 3 h, there are a large number of oxide grains with scales in the range of several 100 nm–1  $\mu$ m, but no evidence of NWs on the surface, as illustrated in Figs. 1(c) and 1(d), where Fig. 1(d) is a magnified image of Fig. 1(c).

Furthermore, the surface compositions of the samples have been analyzed using x-ray photoelectron spectroscopy (XPS). As shown in Fig. 1(e), only peaks for Cu, O, and C can be observed in the survey spectra, thus demonstrating the high purity of the samples. Figures 1(f) and 1(g) represent the narrow spectra of Cu 2*p* and O 1*s*, respectively. For both types of samples, the peaks at about 933.8 and 953.8 eV correspond to the Cu 2*p*<sub>3/2</sub> and Cu 2*p*<sub>1/2</sub>, respectively, which is consistent with the reported data for Cu 2*p* in CuO.<sup>17,18</sup> The absence of peaks at about 932.5 eV rules out the possibility of the presence of a Cu<sub>2</sub>O phase.<sup>19</sup> Moreover, the existence of two shake-up satellites at the high binding energy side of the main peak for Cu 2*p*<sub>3/2</sub> is characteristic of a CuO phase in both sample types.<sup>19</sup> There are two peaks in the XPS spectra for O 1*s*, as shown in Fig. 1(g). The peaks at

about 530.0 eV for both samples are due to the oxygen in the CuO crystal lattice. The other peaks at 532.2 and 531.6 eV, for the NW arrays and granular films, respectively, are caused by hydroxide and/or chemisorbed oxygen on the surfaces.<sup>20</sup> The difference in this peak for the two types of samples can be attributed to their different morphologies, where NW arrays have larger surface areas than granular films. It also can be demonstrated by their Cu:O atomic ratios, which are about 1:1.9 and 1:1.7 for NW arrays and granular films, respectively.

DWCNT films, which were fabricated by chemical vapor deposition, are easily contacted with other materials in a planar configuration.<sup>5,9</sup> First, fully expanded,  $\sim$ 110 nm-thick, DWCNT films were suspended in deionized water. Then, a CuO NW array based on Cu foil was immersed in water to act as the substrate to allow the DWCNT film to be spread upon it. Finally, the sample was dried in air at room temperature. Silver paint was used to connect the upper and lower electrodes to the DWCNT film and Cu substrate, respectively. The upper electrode was separated from the underlying CuO NW array by insulating tape with a window of 2.5 mm by 2.5 mm. The whole structure of the sample is illustrated in Fig. 2(a), where the CNT film forms a

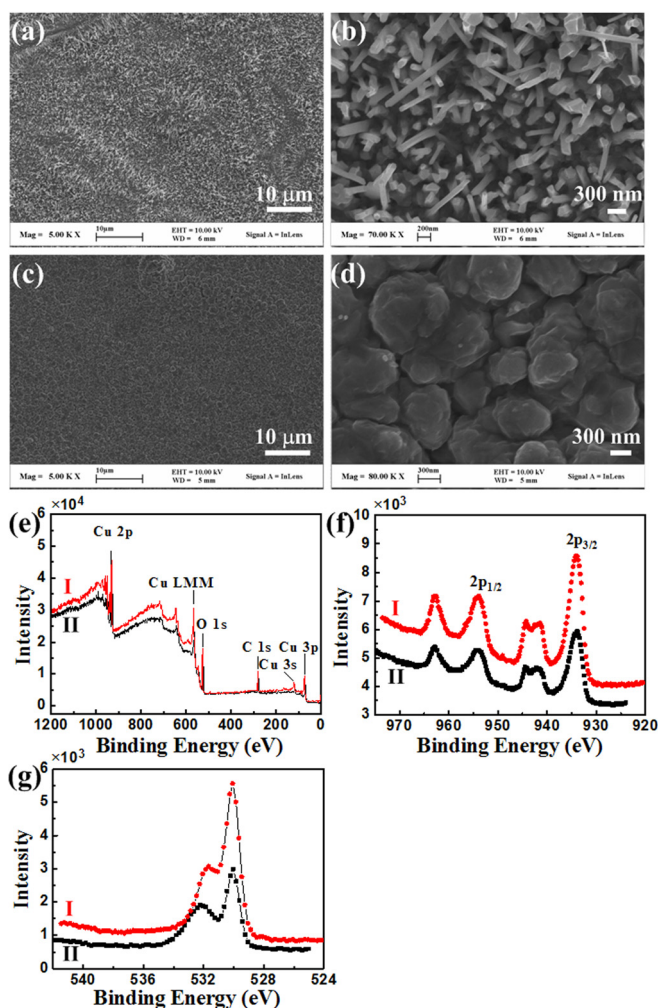


FIG. 1. FESEM images of (a) and (b) a CuO NW array and (c) and (d) a CuO granular film with different magnifications. XPS spectra of the CuO NW array and CuO granular film marked as I and II, respectively: (e) Survey, (f) Cu 2*p*, and (g) O 1*s*.

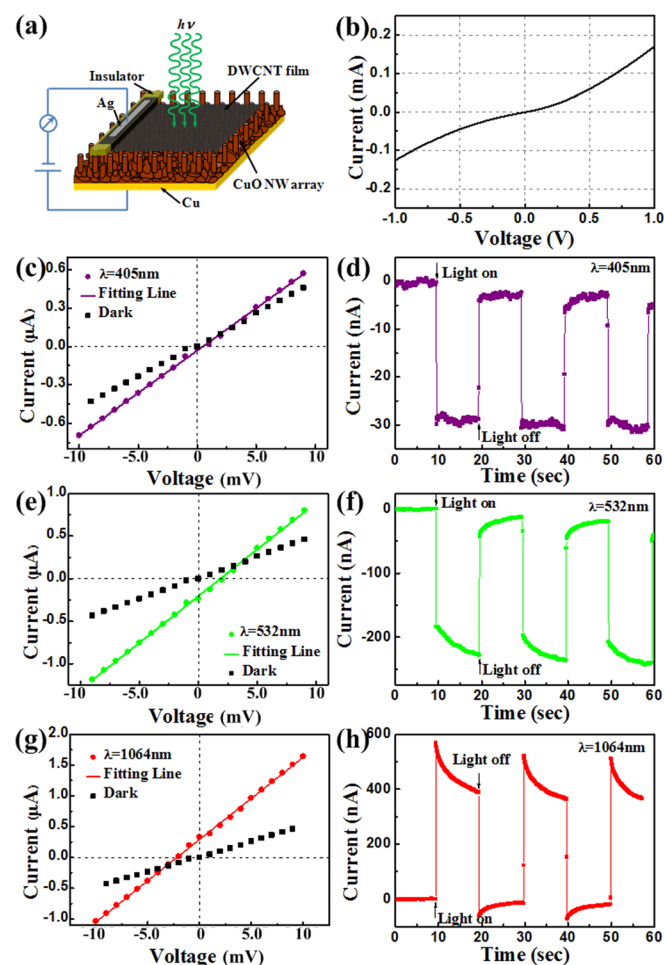


FIG. 2. DWCNT film/CuO NW array heterodimensional contacts: (a) Schematic diagram. (b) *I*-*V* characteristics in the dark within the bias voltage range  $-1.0$  V to  $1.0$  V. [(c), (e), and (g)] *I*-*V* characteristics and [(d), (f), and (h)] photoresponses under illumination with (c) and (d) 405, (e) and (f) 532, and (g) and (h) 1064 nm lasers.

heterodimensional contacts with the CuO NW array and serves as a transparent electrode to allow illumination from this side.

In experiments on the photoelectric properties, three lasers with wavelengths of 405, 532, and 1064 nm, were used as the light sources. A SourceMeter (Keithley 2400) was used to obtain electrical measurements on the devices at room temperature. The forward bias is defined as a positive voltage applied to the Cu substrates. Figure 2(b) plots the current-voltage ( $I$ - $V$ ) characteristics in the bias voltage range of  $-1.0$  V to  $1.0$  V for the CNT film/CuO NW array heterodimensional contacts without illumination. Previous research has demonstrated the ohmic contact between the DWCNTs and the Ag paints electrodes.<sup>9</sup> Thus, the non-linearity of the  $I$ - $V$  curve is primarily due to the barriers induced by the CNT film/CuO NW array and oxide layer/Cu substrate HJs. Given the high conductivity of CNT films and  $p$ -type semiconducting nature of the CuO NWs, an ideal  $I$ - $V$  curve should exhibit the features of two face-to-face Schottky diodes. However, the form of the actual curve, without evidence of rectifying behavior, can be attributed to barrier lowering resulting from impurities at the edges of the electrodes or CNTs. For the bias voltage range of  $-10$  mV to  $10$  mV (step size of 1 mV), Figs. 2(c), 2(e), and 2(g), respectively, show the  $I$ - $V$  characteristics of the CNT film/CuO NW array HJ in the dark and under illumination by 405 nm (10 mW,  $\sim 2$  mm spot size), 532 nm (200 mW,  $\sim 2$  mm spot size), and 1064 nm (100 mW,  $\sim 2$  mm spot size) lasers. In the experiments, the  $I$ - $V$  curves under illumination were obtained after the devices had been irradiated for some time, once they had reached a steady state. Linear-like relationships can be observed between the current and the voltage in all cases. We linearly fitted the  $I$ - $V$  curves under illumination to obtain  $U_{oc}$  and  $I_{sc}$ . Under illumination with 405 and 532 nm lasers, the  $I$ - $V$  curves shift downward, with positive  $U_{oc}$  and negative  $I_{sc}$  of about  $0.48$   $\mu$ V and  $-32$  nA, and  $1.86$  mV and  $-0.20$   $\mu$ A, respectively. Interestingly, when the device was irradiated by the 1064 nm laser, the  $I$ - $V$  curve shifted upward, with a negative  $U_{oc}$  and positive  $I_{sc}$  of about  $-2.18$  mV and  $0.29$   $\mu$ A, respectively. The photoresponse of  $I_{sc}$  under illumination by the three lasers is shown in Figs. 2(d), 2(f), and 2(h), respectively. Clearly, a fast response at the rise and decay edges of  $I_{sc}$  and good repeatability can be observed in all three illumination cases.

Due to the different directions of  $U_{oc}$  and  $I_{sc}$  between the 405 and 532 nm cases and the 1064 nm case, it can be inferred that different mechanisms exist that contribute to the PV effects. The photo-energies of the 405 and 532 nm lasers are both above the bandgap of CuO. A highly conductive CNT film contacted with a CuO NW can result in the formation of a Schottky junction. The ideal band diagram is illustrated in Fig. 3, in which we assume the electron affinity ( $E_c$ ), valence band ( $E_v$ ), and Fermi level ( $E_f$ ) of the  $p$ -type CuO are 3.8, 5.42, and 5.2 eV, respectively, and the  $E_f$  of the CNTs is 4.8 eV, in accordance with the reported data.<sup>8,18</sup> The direction of the built-in electronic field is from the CNTs to the CuO NW arrays. Thus, the photoinduced electron-hole pairs within the CuO under illumination of 405 and 532 nm lasers can be separated by the Schottky junction, where electrons are transported to the CNT film. In actuality,

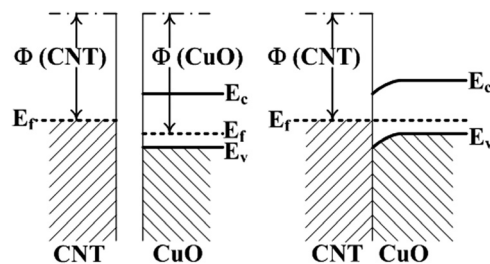


FIG. 3. Energy band diagram between the CNT and the CuO. Left: before contact. Right: after contact.

the obtained  $U_{oc}$  and  $I_{sc}$  are the result of the PV effect which has been partly offset by another Schottky junction with an opposite built-in electric field between the oxide layer and the Cu substrate. Moreover, due to the relatively large intensity of the 532 nm laser, the thermal effect of the laser irradiation can be exhibited by the slow process in the photoresponse of  $I_{sc}$ , as shown in Fig. 2(f).

However, for the 1064 nm case, the photo-energy is slightly lower than the reported bandgap for CuO. If numerous excitations of charge carriers are induced within the CuO by the 1064 nm laser, the directions of  $U_{oc}$  and  $I_{sc}$  should be the same as those shown for the 405 and 532 nm cases. The results of our experiments imply that an alternative mechanism is at play. Here, we proposed a possible mechanism responsible for the observed phenomena. Because the diameter of the DWCNTs is much smaller than that of the CuO NWs, the contacts between them can also be considered as being heterodimensional contacts. Due to the HD effect, for the heterodimensional contacts consisting of same materials but with different dimensions, the transport of net electrons excited by photo or heat from the lower-dimensional material to the neighboring higher-dimensional material is easier than through the reverse direction.<sup>11,21</sup> Therefore, when the contacts composed of different materials with different dimensions are excited by light or heat, both of HJ and HD effects have to be taken into consideration simultaneously. It has been demonstrated that the excitation of non-equilibrium carriers within DWCNTs can take place under illumination by light in the infrared region.<sup>22</sup> Additionally, the heat induced by the radiation of the infrared laser is another possible excitation source for the DWCNTs. Thus, as the results of the excitation within DWCNTs and HD effect, the photo- or thermal-induced electrons with illumination by the 1064 nm laser can transport from the CNT films to the CuO NW arrays, resulting in  $U_{oc}$  and  $I_{sc}$  with reverse directions relative to the 405 and 532 nm cases. The slow decrease in  $I_{sc}$  (Fig. 2(h)) during the irradiation is a result of the complex interplay of different processes, including oxygen photodesorption of the CNTs, sample heating, and surface-assisted carrier recombination within the CNTs or CuO.

In view of the opposite directions of  $U_{oc}$  based on the HJ and HD effects, when the photo-energy is higher than the bandgap of CuO, a competitive relationship for the PV effect should exist in the device between excitation within the CNTs and within the CuO NWs. However, the experimental results show that the photoexcitation within semiconducting CuO NWs dominates the PV effect. This can probably be

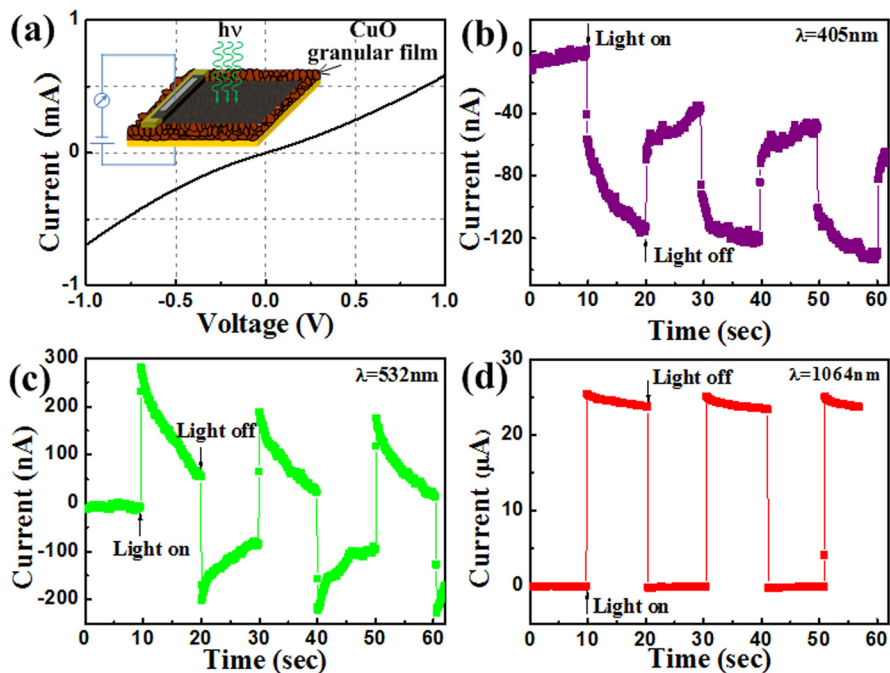


FIG. 4. DWCNT film/CuO granular film heterodimensional contacts: (a)  $I$ - $V$  characteristics in the dark within the bias voltage range  $-1.0$  V to  $1.0$  V. Inset: schematic diagram. Photoresponses under illumination with (b) 405, (c) 532, and (d) 1064 nm lasers.

attributed to two reasons, the first of which is that the large surface of the CuO NW provides photoexcitation with superior performance, thus favoring the HJ effect. The second reason is that the difference in the dimensionality of the CNTs and NWs is not remarkably large, which therefore limits the extent of the HD effect. To further illustrate the two competitive mechanisms, a control experiment was carried out on the device, as illustrated in the inset of Fig. 4(a), in which the CuO granular film rather than NWs was used to contact with the CNT film. In this way, the difference in dimensionality between the CNTs and the CuO grains is larger than that between CNTs and CuO NWs. The effect on the PV effect by the HD is, therefore, expected to be enhanced. The  $I$ - $V$  characteristics within the voltage range  $-1.0$  V to  $1.0$  V without illumination is exhibited in Fig. 4(a), which shows that there is a better contact in the CNT film/CuO granular film HJ than in the CNT film/CuO NWs array HJ. The photoresponse of  $I_{sc}$  under illumination with the same three lasers described *vide supra* are shown in Figs. 4(b)–4(d). The directions of  $I_{sc}$  in the 405 and 1064 nm cases are the same as those in the CNT film/CuO NW array HJs. However, when the device is irradiated by the 532 nm laser  $I_{sc}$  first shows the same direction as in the 1064 nm case and then decreases continuously. Even at the moment when the light is turned off, the equivalent direction as with the 405 nm case of  $I_{sc}$  is exhibited. Moreover, such a tangled process is demonstrated to be reproducible. In this structure, the effect on the PV effect by the enhanced HD effect is increased significantly, such that under illumination with the 532 nm laser there is obvious competition observed between the HD effect and the HJ effect on the PV effect.

In conclusion, CNT film/CuO NW array heterodimensional contacts have been fabricated by the transfer of CNT films onto the top of CuO NW arrays that had been prepared via thermal oxidation. Two mechanisms behind the PV effects have been explored for these structures using 405, 532, and 1064 nm lasers as light sources. When 405 and

532 nm lasers irradiate the devices, which have photoenergies above the bandgap of CuO, photoexcitations within the CuO NW and the HJ effect dominate the PV effects. However, for illumination by the 1064 nm laser, where the photo-energy is lower than the bandgap of CuO, PV effects are considered basing on the excitation within the CNT film and on the HD effect. These two mechanisms and their influence on the PV effects were further demonstrated by control experiments carried out on CNT film/CuO granular film heterodimensional contacts. These results reveal that the heterodimensional contacts exhibit potential applications in the wavelength dependent photosensors.

This work was financially supported by the National Natural Science Foundation of China (Grant Nos. 11004054, 11174172, 50825603, and U1034004), and the Fundamental Research Funds for the Central Universities.

<sup>1</sup>Z. C. Wu, Z. H. Chen, X. Du, J. M. Logan, J. Sippel, M. Nikolou, K. Kamaras, J. R. Reynolds, D. B. Tanner, A. F. Hebard, and A. G. Rinzier, *Science* **305**, 1273 (2004).

<sup>2</sup>Z. R. Li, H. R. Kandel, E. Dervishi, V. Saini, A. S. Biris, A. R. Biris, and D. Lupu, *Appl. Phys. Lett.* **91**, 053115 (2007).

<sup>3</sup>L. B. Hu, D. S. Hecht, and G. Gruner, *Chem. Rev.* **110**, 5790 (2010).

<sup>4</sup>J. Q. Wei, Y. Jia, Q. K. Shu, Z. Y. Gu, K. L. Wang, D. M. Zhuang, G. Zhang, Z. C. Wang, J. B. Luo, A. Y. Cao, and D. H. Wu, *Nano Lett.* **7**, 2317 (2007).

<sup>5</sup>Y. Cao, J. H. He, J. L. Zhu, and J. L. Sun, *Chem. Phys. Lett.* **501**, 461 (2011).

<sup>6</sup>A. Behnam, J. L. Johnson, Y. H. Choi, M. G. Ertosun, A. K. Okay, P. Kapur, K. C. Saraswat, and A. Ural, *Appl. Phys. Lett.* **92**, 243116 (2008).

<sup>7</sup>Y. Jia, J. Q. Wei, K. L. Wang, A. Y. Cao, Q. K. Shu, X. C. Gui, Y. Q. Zhu, D. M. Zhuang, G. Zhang, B. B. Ma, L. D. Wang, W. J. Liu, Z. C. Wang, J. B. Luo, and D. H. Wu, *Adv. Mater.* **20**, 4594 (2008).

<sup>8</sup>L. H. Zhang, Y. Jia, S. S. Wang, Z. Li, C. Y. Ji, J. Q. Wei, H. W. Zhu, K. L. Wang, D. H. Wu, E. Z. Shi, Y. Fang, and A. Y. Cao, *Nano Lett.* **10**, 3583 (2010).

<sup>9</sup>M. J. Yang, J. L. Zhu, W. Liu, and J. L. Sun, *Nano Res.* **4**, 901 (2011).

<sup>10</sup>T. F. Kuo, M. B. Tzolov, D. A. Straus, and J. Xu, *Appl. Phys. Lett.* **94**, 232105 (2009).

<sup>11</sup>J. L. Sun, J. Q. Wei, J. L. Zhu, D. Xu, X. Liu, H. Sun, D. H. Wu, and N. L. Wu, *Appl. Phys. Lett.* **88**, 131107 (2006).

- <sup>12</sup>J. L. Sun, J. Xu, J. L. Zhu, and B. L. Li, *Appl. Phys. A* **91**, 229 (2008).
- <sup>13</sup>F. Marabelli, G. B. Parravicini, and F. Salghetti-Drioli, *Phys. Rev. B* **52**, 1433 (1995).
- <sup>14</sup>X. C. Jiang, T. Herricks, and Y. N. Xia, *Nano Lett.* **2**, 1333 (2002).
- <sup>15</sup>C. H. Xu, C. H. Woo, and S. Q. Shi, *Chem. Phys. Lett.* **399**, 62 (2004).
- <sup>16</sup>A. M. B. Gonçalves, L. C. Campos, A. S. Ferlauto, and R. G. Lacerda, *J. Appl. Phys.* **106**, 034303 (2009).
- <sup>17</sup>C. T. Hsieh, J. M. Chen, H. H. Lin, and H. C. Shih, *Appl. Phys. Lett.* **83**, 3383 (2003).
- <sup>18</sup>P. R. Shao, S. Z. Deng, J. Chen, J. Chen, and N. S. Xu, *J. Appl. Phys.* **109**, 023710 (2011).
- <sup>19</sup>J. Ghijsen, L. H. Tjeng, J. van Elp, H. Eskes, J. Westerink, G. A. Sawatzky, and M. T. Czyzyk, *Phys. Rev. B* **38**, 11322 (1988).
- <sup>20</sup>C. K. Xu, Y. K. Liu, G. D. Xu, and G. H. Wang, *Mater. Res. Bull.* **37**, 2365 (2001).
- <sup>21</sup>J. Xu, J. L. Sun, and J. L. Zhu, *Appl. Phys. Lett.* **91**, 161107 (2007).
- <sup>22</sup>C. Shen, A. H. Brozena, and Y. H. Wang, *Nanoscale* **3**, 503 (2011).